

Research Paper

# CK7 expression associates with the location, differentiation, lymph node metastasis, and the Dukes' stage of primary colorectal cancers

Fei Fei<sup>1,2#</sup>, Chunyuan Li<sup>1,2#</sup>, Yuan Cao<sup>2#</sup>, Kai Liu<sup>3</sup>, Jiaying Du<sup>4</sup>, Yanjun Gu<sup>5</sup>, Xinlu Wang<sup>4</sup>, Yuwei Li<sup>6</sup>, Shiwu Zhang<sup>1,2</sup>✉

1. Nankai University School of Medicine, Nankai University, Tianjin, P.R. China.
2. Department of Pathology, Tianjin Union Medical Center, Tianjin, P.R. China.
3. Tianjin Medical University, Tianjin, P.R. China
4. Graduate School, Tianjin University of Traditional Chinese Medicine, Tianjin, P.R. China
5. Department of pathology, Affiliated Hospital of Logistic University of People's Armed Police Force, Tianjin, P.R. China.
6. Departments of colorectal surgery, Tianjin Union Medical Center, Tianjin, P.R. China

# These authors equally contributed to the paper.

✉ Corresponding author: Shiwu Zhang, M.D., Ph.D., Department of Pathology, Tianjin Union Medical Center, Tianjin, 300121, P.R. China. Nankai University School of Medicine, Nankai University, Tianjin, 300071, P.R. China. Email: zhangshiwu666@aliyun.com. Tel: (086)13652136865; Fax: (86)022-87721989.

© Ivyspring International Publisher. This is an open access article distributed under the terms of the Creative Commons Attribution (CC BY-NC) license (<https://creativecommons.org/licenses/by-nc/4.0/>). See <http://ivyspring.com/terms> for full terms and conditions.

Received: 2018.08.21; Accepted: 2019.04.13; Published: 2019.06.02

## Abstract

**Purpose:** Most colorectal cancers (CRCs) show positive immunohistochemical (IHC) staining for CK20 and negative staining for CK7. However, in clinical settings, some CRCs show positive IHC staining for CK7, and the clinicopathological significance of this needs to be studied. This study investigated the clinicopathological significance of CK7 positivity in CRCs.

**Materials and Methods:** A total of 178 patients with CRC were used to study the clinicopathological significance of CK7 positivity. Western blotting and immunocytochemical (ICC) staining were used to compare the expression levels of CK7 before and after CoCl<sub>2</sub> treatment.

**Results:** CK7 expression was associated with the location, differentiation, lymph node metastasis, and the Dukes' stage of CRCs. CK7 positive cells were mainly distributed at the edge of cancer nests, at the invasion front, as single stromal polyploid giant cancer cells (PGCCs), in tumor buds, in intravascular tumor emboli, and in a micropapillary pattern. Results of ICC staining showed that CK7 expression was almost negative in LoVo and HCT116 before CoCl<sub>2</sub> treatment. After CoCl<sub>2</sub> treatment, the PGCCs and their daughter cells of LoVo and HCT116 yielded positive results in CK7 ICC staining. Results of western blotting also confirmed that there was higher CK7 expression in LoVo and HCT116 after CoCl<sub>2</sub> treatment than in the control.

**Conclusion:** CRC cells expressing CK7 may have strong invasive and metastatic abilities. Some metastasis-related morphological characteristics in CRCs including the invasion front, micropapillary pattern, tumor emboli, and single stromal PGCCs associated with CK7 positive expression.

Key words: cytokeratin 7; colorectal cancer; polyploidy giant cancer cells; tumor budding; micropapillary pattern

## Introduction

Colorectal cancer (CRC) is the second leading cause of death among cancer patients in United States [1] and China [2]. Despite considerable improvements in the treatment of this disease with new therapeutic

agents, the mortality rate is still significant [3]. Characteristics such as infiltration depth, tumor cell differentiation, lymph node or distant metastasis, tumor budding, micropapillary pattern, and

intravascular tumor emboli, etc. [4] are associated with the prognosis of patients with CRC [5]. The Dukes staging system can help clinicians to predict the prognosis of CRCs. However, the Dukes staging is a preliminary evaluation system and patients with the same Dukes' stage can have different prognoses. With the progress in diagnostic molecular pathology, a comprehensive evaluation system including the expression of metastasis-related proteins should be used to guide clinical treatment and predict prognosis.

We first reported that polyploid giant cancer cells (PGCCs) could be induced and purified by  $\text{CoCl}_2$  in vitro and confirmed that PGCCs had the properties of cancer stem cells [6]. In pathology, PGCCs were the key contributors to cellular atypia and were associated with the malignant grade of tumors. In vitro, PGCCs produced daughter cells via asymmetric cell division and these daughter cells had a strong ability to infiltrate and invade by acquiring a mesenchymal phenotype. The number of PGCCs was associated with cancer development, metastasis, chemoresistance, and progression, and there were more PGCCs in cancers of high pathological grades, late stage diseases, recurrent tumors, and after chemotherapy. Furthermore, PGCCs occur mostly in micropapillary carcinomas and tumor buds. Tumor budding and the micropapillary pattern may both be derived from PGCCs and their budding daughter cells [7].

Results of immunocytochemical (ICC) staining and western blot showed that the level of cytokeratin 7 (CK7) expression increased after  $\text{CoCl}_2$  treatment. CK7 was first isolated and purified by Kaba et al. in 1988 [8] and was also named sarcolectin (SCL) because of its high concentration in human osteosarcomas [9]. Cytokeratin 7 (CK7) is specifically expressed in the simple epithelia lining the cavities of internal organs and in transitional epithelium. Epithelial cells of the lung and breast can express CK7, but glandular epithelia of the colon and prostate do not express CK7 [10]. As the CK7 antigen is found in both healthy and neoplastic cells, antibodies against CK7 together with CK20 can be used for immunohistochemistry (IHC) staining to determine the origin of the tumor. Most CRCs show positive IHC staining for CK20 and negative staining for CK7. However, in clinical application, some CRCs show positive IHC staining for CK7. In this study, we provided evidence confirming that tumor cells expressing CK7 were associated with the location, differentiation, lymph node metastasis, and the Dukes' stage of CRCs. In CK7 positive CRCs, the distribution of CK7 positive cells was not uniform. Single stromal PGCCs, cells growing in a

micropapillary pattern, and intravascular tumor emboli were often strongly positive for CK7 IHC staining.

## Materials and Methods

### 1. Patients

The Institutional Review Board of Tianjin Union Medical Center approved this study, and patient anonymity was maintained. We searched the database at the Department of Pathology for cases of CRC. A total of 178 CRC cases were selected and categorized into 2 groups: 71 cases of CK7 positive and 107 cases of CK7 negative CRCs. CK7 positive CRCs from more than one thousand cases in our hospital were used to study the clinicopathological significance and 107 cases of CK7 negative CRCs were used as a randomized controlled comparison. For the CK7 negative group, no tumor cells yielded positive IHC staining results for CK7. For the CK7 positive group, diffuse or focal CK7 positive tumor cells were present in tumor tissue. No patients were treated prior to the radical resection of CRC. All patients were histologically diagnosed as having CRC based on the results of IHC staining. Antibodies against 4 proteins, namely CK20, villin, CDX-2, and cadherin 17, were used to confirm the origin of the cancer as the colon or rectum. Tumor cells positive for at least 3 of these 4 proteins were regarded as originating from the colorectum. These CRCs were all adenocarcinomas excluding signet ring cell carcinomas, mucinous carcinomas and adenocarcinomas with focal mucous differentiation. Muc-2 IHC staining results were negative for these adenocarcinomas and the tumor foci were single.

### 2. Immunohistochemistry (IHC) staining and assessment

IHC staining was performed using the immunohistochemistry autostainer (BenchMark, Roche, Arizona, USA), which has been described in our previous published paper [11]. Briefly, the paraffin-embedded tissue samples were sectioned and deparaffinized using EZ prep solution (BenchMark, Roche, Arizona, USA). The endogenous peroxidase activity was inhibited and the sections were subjected to antigen retrieval in a cell-conditioning solution maintained at 95°C for 30 min. After adding Liquid crystal solution (BenchMark, Roche, Arizona, USA), the sections were incubated at 37°C for 1 h with the appropriate primary antibodies, which included mouse anti-CK7 (MXB Biotechnologies Inc., Fuzhou, China, Kit-0021, 1:100 dilution), rabbit monoclonal anti-CDX2 (MXB Biotechnologies Inc., Fuzhou, China, RMA-0631, 1:100

dilution), mouse anti-CK20 (MXB Biotechnologies Inc., Fuzhou, China, Kit-0025, 1:100 dilution), mouse anti-villin (MXB Biotechnologies Inc., Fuzhou, China, MAB-0540, 1:100 dilution), and rabbit monoclonal anti-cadherin 17 (Zhongshan Golden Bridge Biotechnology, Beijing, China; ZA-0630, 1:200 dilution). Phosphate buffered saline (PBS) was used instead of primary antibody in the negative controls. A secondary antibody was then added to the samples at 37°C for 15 min, and signals were detected using the chromogen 3,3'-diaminobenzidine (DAB). The sections were counterstained with hematoxylin, then dehydrated and mounted on a coverslip. Cytoplasmic immunoreactions for CK7, CK20, villin and cadherin 17 IHC staining were considered as positive and CDX2 IHC staining showed dense positive brown nuclear immunoreactions. For CK20, villin, cadherin 17 and CDX2 IHC staining, immunoreactions appeared in more than 50 percent cells was considered as positive. For CK7 IHC staining, the distribution of CK7 positive cells was not uniform in one slide and only a few of cancer cells (<10%) showed immunoreactions for CK7 IHC staining in some cases, which were also considered as positive.

### 3. Dukes' stage

There are 4 stages in the Dukes' system. Dukes' A indicates that the cancer is in situ or has invaded the submucosa or muscularis propria. Dukes' B indicates that the cancer has invaded through the muscularis propria. Dukes' C indicates that at least one regional lymph node is positive. Dukes' D indicates that the cancer has spread to other parts of the body [12, 13].

### 4. Culture of cancer cell lines and generation of polyploid giant cancer cells

The human colorectal cancer cell lines LoVo and HCT116 were purchased from the American Type Culture Collection (USA) and cultured in RPMI-1640 medium supplemented with 10% fetal bovine serum, 100 U/mL penicillin, and 100 g/mL streptomycin. When the confluence of LoVo and HCT116 cells reached 90%, we treated LoVo with 300  $\mu$ M of CoCl<sub>2</sub> (Sigma-Aldrich, St. Louis, MO, USA) for 72 h and HCT116 with 450  $\mu$ M of CoCl<sub>2</sub> for 48 h. Most diploid LoVo and HCT116 cells died following CoCl<sub>2</sub> treatment, whereas scattered PGCCs survived. A PGCC was defined as a tumor cell with a nucleus at least 3 times larger than that of a diploid tumor cell [6, 12, 14].

### 5. Hematoxylin-eosin staining

Sections of 4  $\mu$ m from formalin-fixed, paraffin-embedded spheroid tissues were deparaffinized, rehydrated, and counterstained with hematoxylin for 1 min and eosin for 2 min. The

sections were then dehydrated and mounted on coverslips.

### 6. Immunocytochemical (ICC) staining

ICC staining using an avidin-biotin-peroxidase complex was performed as previously described [15]. LoVo and HCT116 cells were grown on glass coverslips before and after CoCl<sub>2</sub> treatment until 90% confluence, after which the cells were fixed with 75% ethanol. After washing with PBS, these slides were incubated overnight with mouse anti-CK7 (MXB Biotechnologies Inc., Fuzhou, China, Kit-0021, 1:100 dilution) at 4°C. Finally, the cells were counterstained with hematoxylin and examined under a microscope.

### 7. Western blotting

Western blot analyses were performed as described previously [6, 15]. Total protein of LoVo and HCT116 was extracted before and after treatment and the concentration was determined. The total protein was separated on sodium dodecyl sulfate polyacrylamide gels and transferred to polyvinylidene fluoride membranes (Amersham Hybond-P PVDF Membrane; GE Healthcare). The primary antibody used was CK7, with  $\beta$ -actin (Sigma-Aldrich) used as a control.

### 8. Statistical analysis

The statistical software SPSS 13.0 was used to statistically analyze the data in this study. A  $P < 0.05$  was considered statistically significant. Pearson's chi-square ( $\chi^2$ ) test was used to analyze the differences in location, differentiation, perineural invasion, intravascular tumor emboli, depth of infiltration, lymph node metastasis, and the Dukes' stage between 71 cases of CK7 positive and 107 cases of CK7 negative CRC.

## Results

### 1. Patients

The 178 CRC patients included 71 CK7 positive and 107 CK7 negative cases. The 71 cases of CK7 positive CRC comprised 39 men with a mean age of  $62.18 \pm 11.88$  and 32 women with a mean age of  $61.47 \pm 11.14$ . The 107 cases of CK7 negative CRC comprised 68 men with a mean age of  $63.59 \pm 10.06$  and 39 women with a mean age of  $66.00 \pm 8.63$ .

### 2. Clinical characteristics and findings

According to the criteria by Harbaum L [16], the immunoreactivity of CK7 was categorized as 'negative' (no tumor cells positive), 'focal' (<10% of tumor cells positive), 'moderate' (10-50%) or 'extensive' (>50%). Distinct cytoplasmic immunoreactivity of CK7 was considered positive.

The clinical characteristics of the 178 cases of CRC including 71 CK7 positive (including focal, moderate and extensive positive) and 107 CK7 negative cases are summarized in Table 1. CK7 positivity was correlated with the location, differentiation, lymph node metastasis, and the Dukes' stage. There was no correlation between CK7 positivity and perineural invasion, intravascular tumor thrombus, and the depth of infiltration.

**Table 1.** The differences in location, differentiation, perineural invasion, intravascular tumor emboli, depth of infiltration, lymph node metastasis, and the Dukes' stage between 71 cases of CK7 positive CRC and 107 cases of CK7 negative CRC

		CK7 positive	CK7 negative	$\chi^2$	P
		n	n		
Location	Ascending colon	20	16	4.620	0.032
	Non-ascending colon	51	91		
Differentiation	Well and moderately differentiated	44	86	7.339	0.007
	Poorly differentiated	27	21		
Perineural invasion	Yes	12	13	0.798	0.372
	No	59	94		
Intravascular tumor thrombus	Yes	15	9	0.012	0.914
	No	56	98		
T	T1 + T2	9	18	0.570	0.450
	T3 + T4	62	89		
Lymph node metastasis	Yes	41	39	7.824	0.005
	No	30	68		
Dukes' stage	A + B	30	67	7.137	0.008
	C + D	41	40		

Endoscopy revealed that the tumor masses were located in the colon or rectum. The anatomic site of the tumor in 20 of the 71 cases of CK7 positive CRC and 16 of the 107 cases of CK7 negative CRC was the ascending colon. The difference in the number of cases where the tumor occurred in the ascending colon between CK7 positive and negative CRCs was statistically significant ( $\chi^2 = 4.620$ ,  $P = 0.032$ ). On microscopic examination, well and moderately differentiated CRCs were revealed in 44 (61.97%) of the CK7 positive cases. However, the percentage of well and moderately differentiated tumor was 80.37% (86 of 107) in CK7 negative CRCs. The difference in tumor differentiation between CK7 positive and negative CRCs was statistically significant ( $\chi^2 = 7.339$ ,  $P = 0.007$ ). There was lymph node metastasis in 57.74% of cases (41 of 71) for CK7 positive CRCs compared with 36.45% (39 of 107) for CK7 negative CRCs. The difference in lymph node metastasis between CK7 positive and negative CRCs was statistically significant ( $\chi^2 = 7.824$ ,  $P = 0.005$ ). The percentage of Dukes A and B in CK7 positive CRCs (42.25%) was lower than that (62.62%) in CK7 negative CRCs, and the difference was statistically significant ( $\chi^2 = 7.137$ ,  $P = 0.008$ ).

### 3. CK7 expression was associated with tumor differentiation, metastasis and the formation of PGCCs

As described above, CK7 expression was associated with the location, differentiation, lymph node metastasis, and the Dukes' stage of CRCs. Results of CK7 IHC staining in 71 cases of CRCs showed that well (Fig. 1A-a and -b), moderately (Fig. 1A-c and -d), and poorly differentiated (Fig. 1A-e and -f) CRCs could express CK7. However, there were differences in the distribution of CK7 positive cells in well, moderately, and poorly differentiated CRCs. CK7 positive tumor cells were often diffuse in poorly differentiated CRCs. In well and moderately differentiated CRCs, the distribution of CK7 positive cells was not uniform and was mainly at the edge of the cancer nests (Fig. 1B-a and -b) and the invasion front (Fig. 1B-c and -d). Furthermore, in well and moderately differentiated CRCs with CK7 positivity, single cancer cells with a scattered distribution almost always yielded positive IHC staining results for CK7 and only some of the cells in the cancer nests yielded positive results for CK7 (Fig. 1B-e and -f). In poorly differentiated CRCs, almost all tumor cells were CK7 positive (Fig. 1B-g and -h).

Using the definition of PGCCs established by Zhang et al. [6], PGCCs with giant or multiple nuclei could be observed in CRCs, with some single PGCCs located in the stroma. Next, we evaluated the significance between single stromal PGCCs and CK7 IHC staining in CRCs. The prognosis of CRC patients has been associated with the infiltration depth, tumor cell differentiation, and lymph node or distant metastasis. Tumor budding is an increasingly important morphological feature which correlates with lymph node or distant metastasis in CRCs [7]. We previously reported that PGCCs induced by  $\text{CoCl}_2$  could generate daughter cells with strong migratory and invasive abilities. Single stromal PGCCs with budding daughter cells were associated with lymph node metastasis in CRCs [12]. PGCCs were observed in CRCs (Fig. 2A-a) and these PGCCs yielded positive IHC staining results for CK7 (Fig. 2A-b). Figures 2A-c and -d show a single PGCC in the stroma that yielded positive results for CK7 IHC staining. We previously reported that the number of PGCCs was associated with CRC differentiation [12] and a higher number of PGCCs was observed in poorly differentiated CRCs than in well and moderately differentiated CRCs. Figure 2A-e shows that there were many single PGCCs in poorly differentiated CRCs and these PGCCs could generate daughter cells. Both PGCCs and their daughter cells yielded positive IHC staining results for CK7 (Fig. 2A-f). Furthermore, micropapillary pattern and intravascular tumor

emboli in carcinomas were associated with a greater frequency of lymphovascular invasion, lymph node metastases, and poor prognosis [17]. In well and moderately differentiated CRCs, the distribution of CK7 positive cells was not uniform and only a few tumor cells yielded positive IHC staining results for CK7. However, tumor cells within the intravascular tumor emboli (Fig. 2B-a and -b), micropapillary pattern (Fig. 2B-c and -d), and lymph node metastases (Fig. 2B-e and -f) always showed CK7 positive staining, which showed that CK7 positive tumor cells had strong infiltration and invasion abilities.

#### 4. Formation of PGCCs in response to CoCl<sub>2</sub> treatment

PGCCs of LoVo and HCT116 were induced by CoCl<sub>2</sub> treatment. The control LoVo (Fig. 3A-a) and HCT116 (Fig. 3A-d) cells were irregular in shape.

Scattered PGCCs were observed in control LoVo and HCT116 before CoCl<sub>2</sub> treatment. After treatment with CoCl<sub>2</sub>, PGCCs could be clearly visualized after removing floating dead cells (Fig. 3A-b and -e). After recovery from CoCl<sub>2</sub> treatment, PGCCs could generate daughter cells via budding (Fig. 3A-c and -f).

#### 5. CK7 expression was increased in LoVo and HCT116 after CoCl<sub>2</sub> treatment

PGCCs with budding daughter cells and the control cells were cultured on coverslips. We performed CK7 ICC staining in LoVo and HCT116 before and after CoCl<sub>2</sub> treatment. Results of ICC staining showed that the control LoVo (Fig. 3B-a) and HCT116 (Fig. 3B-d) cells showed negative staining results for CK7. The scattered PGCCs in control LoVo and HCT116 yielded positive ICC staining results for CK7. When LoVo and HCT116 were treated with

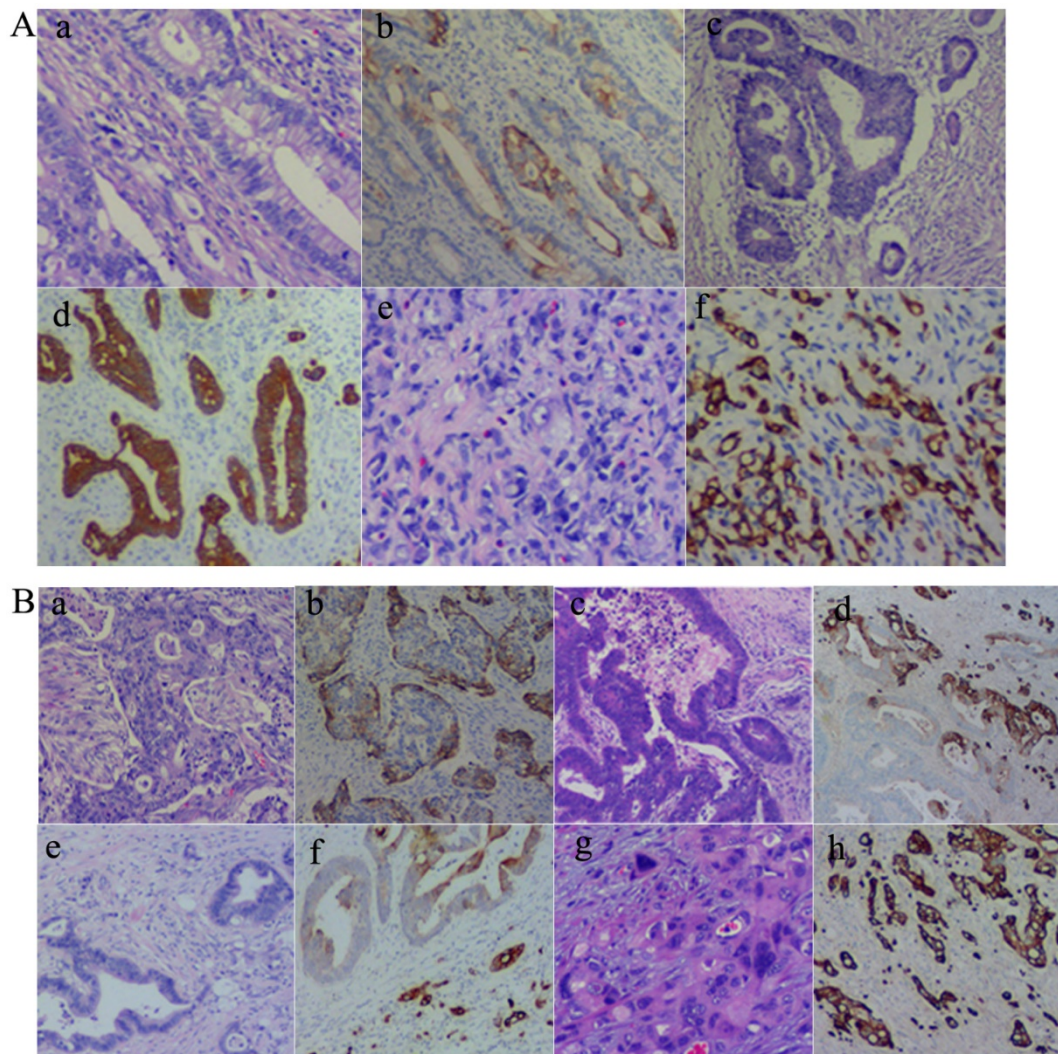


**Figure 1.** A. CK7 expression in CRCs with different differentiation statuses. (a) Well differentiated CRCs (H&E, 10 $\times$ ). (b) CK7 positive staining of (a) (IHC, 10 $\times$ ). (c) Moderately differentiated CRCs (H&E, 10 $\times$ ). (d) CK7 positive staining of (c) (IHC, 10 $\times$ ). (e) Poorly differentiated CRCs (H&E, 10 $\times$ ). (f) CK7 positive staining of (e) (IHC, 10 $\times$ ). B. Distribution of CK7 positive cells in CRCs. (a) H&E staining of CRC with solid nested distribution (H&E, 10 $\times$ ). (b) CK7 IHC staining of (a) (IHC, 10 $\times$ ). (c) H&E staining of CRC at the invasion front (H&E, 10 $\times$ ). (d) CK7 IHC staining of (c) (IHC, 10 $\times$ ). (e) H&E staining of well differentiated CRC with scattered distribution of single cancer cells (H&E, 10 $\times$ ). (f) CK7 IHC staining of (e) (IHC, 10 $\times$ ). (g) H&E staining of poorly differentiated CRC (H&E, 10 $\times$ ). (h) CK7 IHC staining of (g) (IHC, 10 $\times$ ).

CoCl<sub>2</sub>, the surviving PGCCs recovered from CoCl<sub>2</sub> treatment and generated daughter cells. PGCCs and some daughter cells yielded positive ICC staining results for CK7 (Fig. 3B-c and -f). CK7 was localized in the cytoplasm of PGCCs and their daughter cells. LoVo and HCT116 were treated with CoCl<sub>2</sub> 3 times. When the PGCCs of LoVo and HCT116 recovered from CoCl<sub>2</sub> treatment and generated daughter cells, these cells were harvested for western blot analysis. Western blot analysis confirmed that CK7 expression was increased in PGCCs and their budding daughter cells compared to control LoVo and HCT116 (Fig. 3C).

## Discussion

Tumor cell invasion and metastasis are key factors for tumor recurrence and patient prognosis. The clinical staging of CRC is mainly based on the invasive depth of tumor cells and the presence of metastasis. In the current study, according to the results of CK7 IHC staining, 178 CRC cases were categorized into 2 groups: CK7 positive and CK7 negative. We provided evidence showing that CK7 positivity was associated with the location,

differentiation, lymph node metastasis, and the Dukes' stage of CRCs. For the CK7 negative group, no tumor cells yielded positive IHC staining results for CK7. For the CK7 positive group, diffuse or focal CK7 positive tumor cells were present in tumor tissue. The diffuse distribution of CK7 positive tumor cells was often present in poorly differentiated CRCs. In well and moderately differentiated CRCs, the distribution of CK7 positive cells was not uniform and was mainly at the edge of cancer nests, the invasion front, tumor buds [16], single stromal PGCCs, intravascular tumor emboli, and cells growing in a micropapillary pattern. Furthermore, CK7 positivity is associated with the anatomic site of the tumor and there were more CK7 positive cases in the ascending colon. Tumor location of CRC is a fundamental factor affecting the pathways to metastasis and different anatomic site of CRC has different macroscopic properties, different dominant pathways to relapse, and different treatment methods [18]. Ascending colon cancer exhibits different histological and molecular characteristics compared with the left-side colon cancer [19].

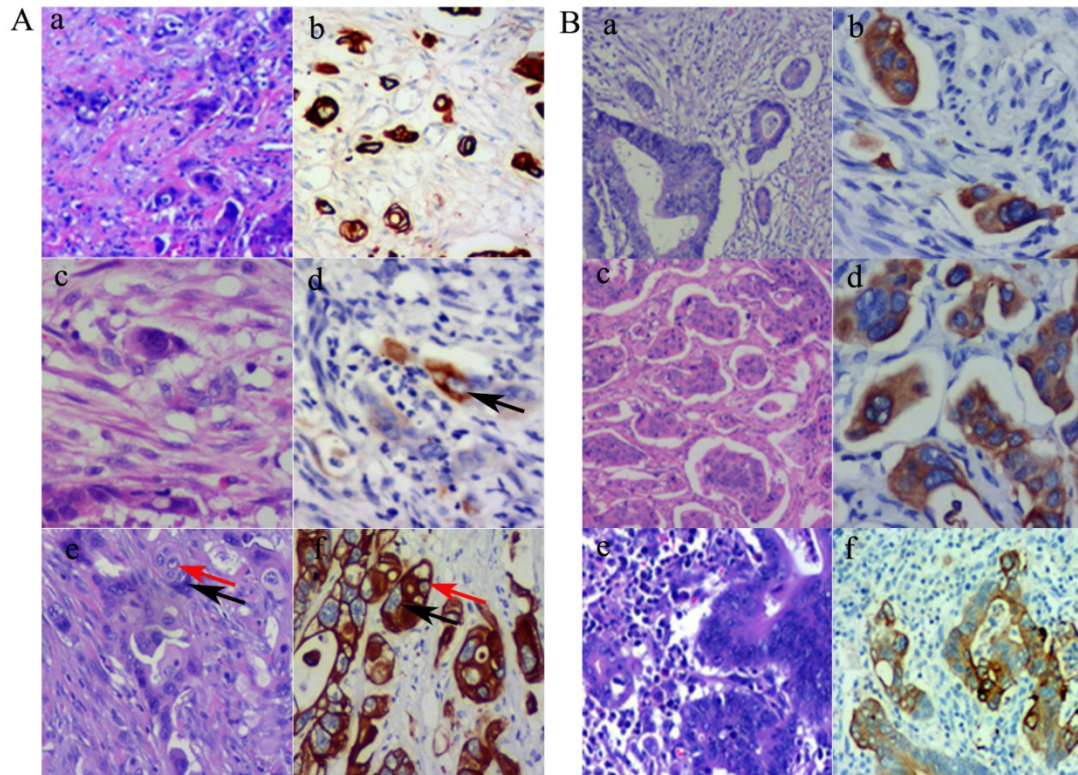


**Figure 2.** A. PGCCs and their generated daughter cells were CK7 positive. (a). PGCCs in CRC (H&E, 10×). (b) PGCCs in CRC yielded positive IHC staining results for CK7 (IHC, 10×). (c) Single stroma PGCCs in CRC (H&E, 10×). (d) Single stroma PGCCs yielded positive IHC staining results for CK7 (black arrows) (IHC, 10×). (e) PGCCs (black arrows) with their generated daughter cells (red arrows) (H&E, 10×). (f) Both PGCCs (black arrows) and their generated daughter cells (red arrows) yielded positive IHC staining results for CK7. (a) Tumor emboli in CRCs (H&E, 10×). (b) Tumor emboli of (a) yielded positive results for CK7 (IHC, 10×). (c) Cells growing in a micropapillary pattern in CRCs (H&E, 10×). (d) Cells growing in a micropapillary pattern (a) yielded positive results for CK7 (IHC, 10×). (e) Lymph node metastatic tumor cells in CRCs (H&E, 10×). (f) Lymph node metastatic tumor cells of (a) yielded positive results for CK7 (IHC, 10×).

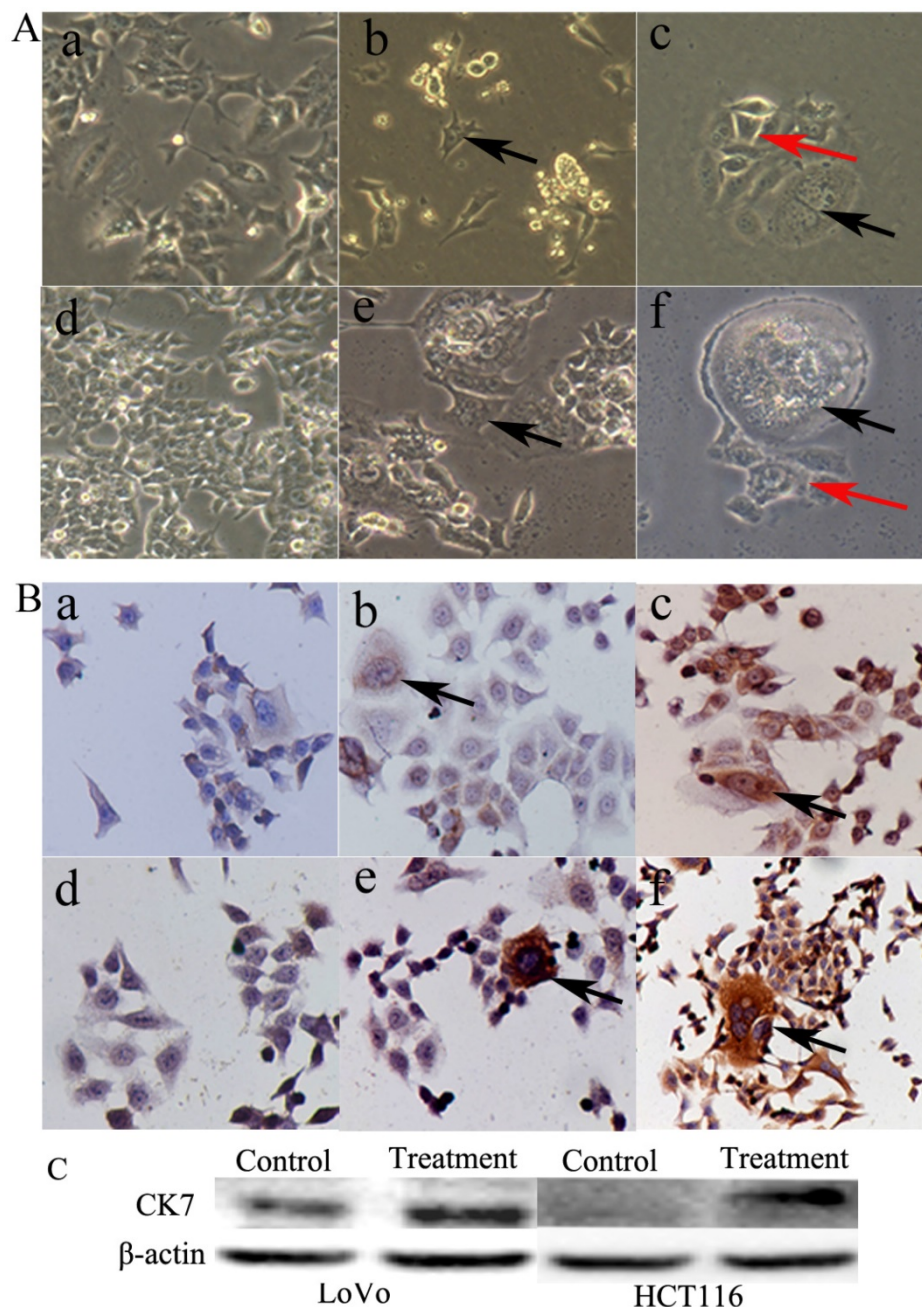


**Figure 3.** A. Morphological characteristics of LoVo and HCT116 before and after CoCl<sub>2</sub> treatment. (a) Morphological characteristics of LoVo cells before CoCl<sub>2</sub> treatment (10×). (b) LoVo PGCCs survived the treatment of 300 μM CoCl<sub>2</sub> for 48 h (black arrows, 10×). (c) LoVo PGCCs (black arrows) generated daughter cells (red arrows) after CoCl<sub>2</sub> treatment (10×). (d) Morphological characteristics of HCT116 cells before CoCl<sub>2</sub> treatment (10×). (e) HCT116 PGCCs survived the treatment of 300 μM CoCl<sub>2</sub> for 48 h (black arrows, 10×). (f) HCT116 PGCCs (black arrows) generated daughter cells (red arrows) after CoCl<sub>2</sub> treatment (10×). B. CK7 IHC staining of LoVo and HCT116 before and after CoCl<sub>2</sub> treatment. (a) Control LoVo cells yielded negative IHC staining results for CK7 (IHC, 10×). (b) Few PGCCs from LoVo (black arrows) yielded positive IHC staining results for CK7 before CoCl<sub>2</sub> treatment (IHC, 10×). (c) More PGCCs of LoVo (black arrows) were strongly positive for CK7 IHC staining after CoCl<sub>2</sub> treatment (IHC, 10×). (d) Control HCT116 cells yielded negative IHC staining results for CK7 (IHC, 10×). (e) Few PGCCs from HCT116 (black arrows) yielded positive IHC staining results for CK7 before CoCl<sub>2</sub> treatment (IHC, 10×). (f) PGCCs of HCT116 (black arrows) were strongly positive for CK7 IHC staining after CoCl<sub>2</sub> treatment (IHC, 10×).

We have proven that PGCCs could be induced in vitro and generate daughter cells via budding [20-22]. ICC and western blotting also confirmed that LoVo and HCT116 PGCCs and their daughter cells had higher CK7 expression than the control cells. PGCCs were often located at the invasion front, which is the boundary of tumor infiltration into normal tissue. We previously reported that there were more PGCCs in poorly differentiated CRCs than in well and

moderately differentiated CRCs [12]. Single stromal PGCCs were associated with tumor metastasis in CRCs and ovarian carcinomas [23], and tumors with single stromal PGCCs have been shown to be highly aggressive. Lv et al. reported that high-grade ovarian carcinoma had more single stromal PGCCs than low-grade ovarian carcinoma [23, 24]. Single stromal PGCCs with budding were also observed in CRCs [12].

There is a close association between single stromal PGCCs, tumor budding, and micropapillary pattern. Understanding this association can help us to further explore the basis of tumor metastasis and patient prognosis. Tumor cell morphology at the invasion front is different from that in the tumor center. We previously reported that tumor budding was due to single stromal PGCCs or daughter cells budding from PGCCs [12]. The budding daughter cells with strong migratory and invasive abilities can easily metastasize to lymph nodes or distant organs by expressing epithelial mesenchymal transition (EMT) related proteins.

Furthermore, the micropapillary pattern is formed by small clusters of tumor cells without vessels and stromal cells in the middle of a tumor cluster [25]. It has been reported to appear in cancers of the breast, bladder, lung, pancreas, ovary, urothelial tract, and stomach [26-29] and is associated with tumor differentiation, lymph node and distant metastasis, and lymphovascular tumor emboli [7, 17]. PGCCs appear in most of micropapillary carcinoma patterns and tumor buds [7, 12, 30]. A similar morphological structure of the micropapillary pattern called cancer organotypic structure, which consists of PGCCs and their daughter cells, could be induced by paclitaxel in the breast cancer cell line MCF-7 [15]. Tumor budding may have the same origin as the micropapillary pattern, and they may both be derived from PGCCs and their budding daughter cells, which show strong invasive abilities. Tumor budding is associated with lymph node or distant metastasis and patient prognosis in CRCs [31, 32]. Tumor budding was first described by Imai who noticed cells sprouting from the edge of tumor nests [33] and referred to them as clusters of cancer cells composed of fewer than 5 cancer cells. Similar to single stromal PGCCs, tumor budding was also mainly located at the invasion front [34-36]. Furthermore, the number of tumor buds was positively correlated with the rate of tumor metastasis in CRCs, which was proven by Hase et al. [37] and Ueno et al [38-41].

CK7 is a protein that is encoded by the KRT7 gene in humans and is specifically expressed in the simple epithelia lining the cavities of internal organs and in the gland ducts and blood vessels. In general, the epithelial cells of the lung and breast can express CK7, but glandular epithelia of the colon and prostate do not contain CK7. In this study, we confirmed that some CRCs could express CK7 and positive CK7 IHC staining in CRCs was associated with tumor location, differentiation, and lymph node metastasis. It was reported that CK7 is present in fetal cells and is expressed in the metaplastic and neoplastic epithelial cells of the stomach; CK7 expression in the stomach

could be defined by a fetal-like, dedifferentiated cellular phenotype during the development of metaplasia and neoplasia [42]. CK20 can be used to identify a range of adenocarcinoma arising from colorectum, transitional cell carcinomas, but is absent in lung cancer, prostate cancer, and non-mucinous ovarian cancer. It is often used in combination with antibodies to CK7 to distinguish different types of adenocarcinoma [10]. Our previous studies have confirmed that PGCCs had the properties of cancer stem cells [6, 12, 14, 15]. Results of ICC staining showed that PGCCs and their daughter cells were strongly positive for CK7. Tumor buds and the micropapillary pattern were composed of PGCCs and their daughter cells, which also yielded positive IHC staining results for CK7. Furthermore, hyperplastic polyps and serrated adenoma in the colorectum yielded positive staining results for CK7 and canalicular adenoma yielded negative results for CK20. Hyperplastic polyp and serrated adenoma have a high rate of canceration, which may be correlated with CK7 expression, a marker of dedifferentiated epithelial cells [43]. It is reported that CK7 was positive associated with ulcerative colitis (UC)-associated neoplasms [44]. In serrated polyps from inflammatory bowel disease patients, dysplasia grade correlated with BRAF and KRAS mutation status, prevalent conventional neoplasia, and rates of advanced neoplasia development [45]. CRCs that evolve through serrated pathways are over-represented in the proximal colon [43, 46], which is in accordance with CK7 expression associated with the location of CRCs. Thirdly, Landau MS et al. reported that CK7 expression related with the status of BRAF and microsatellite stability and there was more expression of CK7 in BRAF-mutated microsatellite stable (MSS) colorectal carcinoma compared to both BRAF-mutated high-level microsatellite instability (MSI-H) colorectal carcinoma and BRAF wild-type MSS colorectal carcinoma [47].

## Conclusion

Our data demonstrated that CK7 positivity was associated with the location, differentiation, lymph node metastasis, and the Dukes' stage of CRCs. CK7 positive cells were not uniformly distributed and mainly were distributed at the edge of cancer nests, the invasion front, tumor buds, as single stromal PGCCs, in intravascular tumor emboli, and in the micropapillary pattern. However, further studies are required to elucidate the detailed molecular mechanisms of CK7 positivity and its association with tumor lymph node metastasis and regulation of signal pathways.

## Abbreviations

CK7: Cytokeratin 7; PGCCs: polyploid giant cancer cells; IHC staining: immunohistochemical staining; ICC staining: immunocytochemical staining; CoCl<sub>2</sub>: cobalt chloride; CRC: colorectal cancer; H&E: hematoxylin-eosin.

## Acknowledgements

This work was supported in part by grants from the National Natural Science Foundation of China (#81472729 and #81672426), and the foundation of committee on science and technology of Tianjin (17ZXMFSY00120 and 17YFZCSY00700), and foundation of Tianjin Union Medical Center (2017YJ009).

## Competing Interests

The authors have declared that no competing interest exists.

## References

- Jemal A, Siegel R, Ward E, Hao Y, Xu J, Murray T, et al. Cancer statistics, 2008. *CA: a cancer journal for clinicians*. 2008; 58: 71-96.
- Bray F, Ferlay J, Soerjomataram I, Siegel RL, Torre LA, Jemal A. Global cancer statistics 2018: GLOBOCAN estimates of incidence and mortality worldwide for 36 cancers in 185 countries. *CA: a cancer journal for clinicians*. 2018.
- Segal NH, Saltz LB. Evolving treatment of advanced colon cancer. *Annual review of medicine*. 2009; 60: 207-19.
- Dukes CE, Bussey HJ. The spread of rectal cancer and its effect on prognosis. *Br J Cancer*. 1958; 12: 309-20.
- Guzinska-Ustymowicz K. MMP-9 and cathepsin B expression in tumor budding as an indicator of a more aggressive phenotype of colorectal cancer (CRC). *Anticancer Res*. 2006; 26: 1589-94.
- Zhang S, Mercado-Uribe I, Xing Z, Sun B, Kuang J, Liu J. Generation of cancer stem-like cells through the formation of polyploid giant cancer cells. *Oncogene*. 2014; 33: 116-28.
- Zhang S, Zhang D, Yang Z, Zhang X. Tumor Budding, Micropapillary Pattern, and Polyploidy Giant Cancer Cells in Colorectal Cancer: Current Status and Future Prospects. *Stem cells international*. 2016; 2016: 4810734.
- Glass C, Fuchs E. Isolation, sequence, and differential expression of a human K7 gene in simple epithelial cells. *The Journal of cell biology*. 1988; 107: 1337-50.
- Kaba A, Jiang PH, Chany-Fournier F, Chany C. Sarcolectin (SCL): structure and expression of the recombinant molecule. *Biochimie*. 1999; 81: 709-15.
- Lyn J, Wang Y, Wang F, Shen M, Zhou X. Diagnostic value of SATB2, CK7 and CK20 in colorectal cancer. *Zhonghua bing li xue za zhi Chinese journal of pathology*. 2015; 44: 578-81.
- Li Y, Yu Y, Li S, Zhang M, Zhang Z, Zhang X, et al. Isobaric tags for relative and absolute quantification-based proteomic analysis that reveals the roles of progesterone receptor, inflammation, and fibrosis for slow-transit constipation. *Journal of gastroenterology and hepatology*. 2018; 33: 385-92.
- Zhang D, Yang X, Yang Z, Fei F, Li S, Qu J, et al. Daughter Cells and Erythroid Cells Budding from PGCCs and Their Clinicopathological Significances in Colorectal Cancer. *Journal of Cancer*. 2017; 8: 469-78.
- Abdel-Rahman O. Revisiting Dukes' paradigm; some node positive colon cancer patients have better prognosis than some node negative patients. *Clinical & translational oncology : official publication of the Federation of Spanish Oncology Societies and of the National Cancer Institute of Mexico*. 2018; 20: 794-800.
- Zhang S, Mercado-Uribe I, Hanash S, Liu J. iTRAQ-based proteomic analysis of polyploid giant cancer cells and budding progeny cells reveals several distinct pathways for ovarian cancer development. *PLoS one*. 2013; 8: e80120.
- Zhang S, Mercado-Uribe I, Liu J. Tumor stroma and differentiated cancer cells can be originated directly from polyploid giant cancer cells induced by paclitaxel. *International journal of cancer Journal international du cancer*. 2014; 134: 508-18.
- Harbaum L, Pollheimer MJ, Kornprat P, Lindtner RA, Schlemmer A, Rehak P, et al. Keratin 7 expression in colorectal cancer—break of nature or significant finding? *Histopathology*. 2011; 59: 225-34.
- Tang T, Zhang X, Zhao L, Cao Y, Xiao L, Wang R. Relationship between colorectal adenocarcinoma with invasive micropapillary carcinoma component and lymph node metastasis. *Zhonghua Binglixue Zazhi*. 2013; 42: 525-9.
- Bauer KM, Hummon AB, Buechler S. Right-side and left-side colon cancer follow different pathways to relapse. *Molecular carcinogenesis*. 2012; 51: 411-21.
- Baran B, Mert Ozupek N, Yerli Tetik N, Acar E, Bekcioglu O, Baskin Y. Difference Between Left-Sided and Right-Sided Colorectal Cancer: A Focused Review of Literature. *Gastroenterology research*. 2018; 11: 264-73.
- Lv H, Shi Y, Zhang L, Zhang D, Liu G, Yang Z, et al. Polyploid giant cancer cells with budding and the expression of cyclin E, S-phase kinase-associated protein 2, stathmin associated with the grading and metastasis in serous ovarian tumor. *BMC cancer*. 2014; 14: 576.
- Fei F, Zhang D, Yang Z, Wang S, Wang X, Wu Z, et al. The number of polyploid giant cancer cells and epithelial-mesenchymal transition-related proteins are associated with invasion and metastasis in human breast cancer. *Journal of experimental & clinical cancer research : CR*. 2015; 34: 158.
- Zhang S, Mercado-Uribe I, Sood A, Bast RC, Liu J. Coevolution of neoplastic epithelial cells and multilineage stroma via polyploid giant cells during immortalization and transformation of mullerian epithelial cells. *Genes & cancer*. 2016; 7: 60-72.
- Lv H, Y S, L Z, D Z, G L, Z Y, et al. Polyploid giant cancer cells with budding and the expression of cyclin E, S-phase kinase-associated protein 2, stathmin associated with the grading and metastasis in serous ovarian tumor. *BMC Cancer*. 2014; 14: 576-85.
- Qu Y, Zhang L, Rong Z, He T, Zhang S. Number of glioma polyploid giant cancer cells (PGCCs) associated with vasculogenic mimicry formation and tumor grade in human glioma. *J Exp Clin Cancer Res*. 2013; 32: 75.
- Vardar E, Yardim BG, Vardar R, Olmez M. Primary Gastric Invasive Micropapillary Carcinoma: A Case Report. *Turk Patoloji Derg*. 2015; 31: 219-22.
- Yang YL, Liu BB, Zhang X, Fu L. Invasive Micropapillary Carcinoma of the Breast: An Update. *Arch Pathol Lab Med*. 2016; 140: 799-805.
- Bertz S, Wach S, Taubert H, Merten R, Krause FS, Schick S, et al. Micropapillary morphology is an indicator of poor prognosis in patients with urothelial carcinoma treated with transurethral resection and radiochemotherapy. *Virchows Arch*. 2016.
- Cao Y, Zhu LZ, Jiang MJ, Yuan Y. Clinical impacts of a micropapillary pattern in lung adenocarcinoma: a review. *Oncotargets Ther*. 2016; 9: 149-58.
- Badal RK, Bal A, Das A, Singh G. Invasive Micropapillary Carcinoma of the Breast: Immunophenotypic Analysis and Role of Cell Adhesion Molecules (CD44 and E-Cadherin) in Nodal Metastasis. *Appl Immunohistochem Mol Morphol*. 2016; 24: 151-8.
- Verdu M, Roman R, Calvo M, Rodon N, Garcia B, Gonzalez M, et al. Clinicopathological and molecular characterization of colorectal micropapillary carcinoma. *Modern pathology : an official journal of the United States and Canadian Academy of Pathology, Inc*. 2011; 24: 729-38.
- Manjula BV, Augustine S, Selvam S, Mohan AM. Prognostic and predictive factors in gingivo buccal complex squamous cell carcinoma: role of tumor budding and pattern of invasion. *Indian J Otolaryngol Head Neck Surg*. 2015; 67: 98-104.
- Landau MS, Hastings SM, Foxwell TJ, Luketich JD, Nason KS, Davison JM. Tumor budding is associated with an increased risk of lymph node metastasis and poor prognosis in superficial esophageal adenocarcinoma. *Modern pathology : an official journal of the United States and Canadian Academy of Pathology, Inc*. 2014; 27: 1578-89.
- Sordat I, Rousselle P, Chaubert P, Petermann O, Aberdam D, Bosman FT, et al. Tumor cell budding and laminin-5 expression in colorectal carcinoma can be modulated by the tissue micro-environment. *International journal of cancer Journal international du cancer*. 2000; 88: 708-17.
- Graham RP, Vierkant RA, Tillmans LS, Wang AH, Laird PW, Weisenberger DJ, et al. Tumor Budding in Colorectal Carcinoma: Confirmation of Prognostic Significance and Histologic Cutoff in a Population-based Cohort. *Am J Surg Pathol*. 2015; 39: 1340-6.
- O'Connor K, Li-Chang HH, Kalloger SE, Peixoto RD, Webber DL, Owen DA, et al. Tumor budding is an independent adverse prognostic factor in pancreatic ductal adenocarcinoma. *Am J Surg Pathol*. 2015; 39: 472-8.
- Angadi PV, Patil PV, Hallikeri K, Mallapur MD, Hallikerimath S, Kale AD. Tumor budding is an independent prognostic factor for prediction of lymph node metastasis in oral squamous cell carcinoma. *International journal of surgical pathology*. 2015; 23: 102-10.
- Hase K, Shatney C, Johnson D, Trollope M, Vierra M. Prognostic value of tumor "budding" in patients with colorectal cancer. *Diseases of the colon and rectum*. 1993; 36: 627-35.
- Ueno H, Mochizuki H, Hashiguchi Y, Shimazaki H, Aida S, Hase K, et al. Risk factors for an adverse outcome in early invasive colorectal carcinoma. *Gastroenterology*. 2004; 127: 385-94.
- Ueno H, Mochizuki H, Hatsuse K, Hase K, Yamamoto T. Indicators for treatment strategies of colorectal liver metastases. *Annals of surgery*. 2000; 231: 59-66.
- Ueno H, Murphy J, Jass JR, Mochizuki H, Talbot IC. Tumour 'budding' as an index to estimate the potential of aggressiveness in rectal cancer. *Histopathology*. 2002; 40: 127-32.
- Ueno H, Price AB, Wilkinson KH, Jass JR, Mochizuki H, Talbot IC. A new prognostic staging system for rectal cancer. *Annals of surgery*. 2004; 240: 832-9.

42. Kirchner T, Muller S, Hattori T, Mukaisyo K, Papadopoulos T, Brabletz T, et al. Metaplasia, intraepithelial neoplasia and early cancer of the stomach are related to dedifferentiated epithelial cells defined by cytokeratin-7 expression in gastritis. *Virchows Archiv : an international journal of pathology*. 2001; 439: 512-22.
43. Jass JR, Young J, Leggett BA. Hyperplastic polyps and DNA microsatellite unstable cancers of the colorectum. *Histopathology*. 2000; 37: 295-301.
44. Tatsumi N, Kushima R, Vieth M, Mukaisho K, Kakinoki R, Okabe H, et al. Cytokeratin 7/20 and mucin core protein expression in ulcerative colitis-associated colorectal neoplasms. *Virchows Archiv : an international journal of pathology*. 2006; 448: 756-62.
45. Ko HM, Harpaz N, McBride RB, Cui M, Ye F, Zhang D, et al. Serrated colorectal polyps in inflammatory bowel disease. *Modern pathology : an official journal of the United States and Canadian Academy of Pathology, Inc*. 2015; 28: 1584-93.
46. Jass JR. Molecular heterogeneity of colorectal cancer: Implications for cancer control. *Surgical oncology*. 2007; 16 Suppl 1: S7-9.
47. Landau MS, Kuan SF, Chiosea S, Pai RK. BRAF-mutated microsatellite stable colorectal carcinoma: an aggressive adenocarcinoma with reduced CDX2 and increased cytokeratin 7 immunohistochemical expression. *Human pathology*. 2014; 45: 1704-12.